AIP | APL Materials

Research Update: Strategies for improving the stability of perovskite solar cells

Severin N. Habisreutinger, David P. McMeekin, Henry J. Snaith, and Robin J. Nicholas

Citation: APL Mater. **4**, 091503 (2016); doi: 10.1063/1.4961210
View online: http://dx.doi.org/10.1063/1.4961210
View Table of Contents: http://scitation.aip.org/content/aip/journal/aplmater/4/9?ver=pdfcov
Published by the AIP Publishing

APL MATERIALS **4**, 091503 (2016)

Research Update: Strategies for improving the stability of perovskite solar cells

Severin N. Habisreutinger,[a] David P. McMeekin, Henry J. Snaith, and Robin J. Nicholas
Department of Physics, Clarendon Laboratory, University of Oxford, Parks Road, Oxford OX1 3PU, United Kingdom

(Received 30 June 2016; accepted 3 August 2016; published online 25 August 2016)

The power-conversion efficiency of perovskite solar cells has soared up to 22.1% earlier this year. Within merely five years, the perovskite solar cell can now compete on efficiency with inorganic thin-film technologies, making it the most promising of the new, emerging photovoltaic solar cell technologies. The next grand challenge is now the aspect of stability. The hydrophilicity and volatility of the organic methylammonium makes the work-horse material methylammonium lead iodide vulnerable to degradation through humidity and heat. Additionally, ultraviolet radiation and oxygen constitute stressors which can deteriorate the device performance. There are two fundamental strategies to increasing the device stability: developing protective layers around the vulnerable perovskite absorber and developing a more resilient perovskite absorber. The most important reports in literature are summarized and analyzed here, letting us conclude that any long-term stability, on par with that of inorganic thin-film technologies, is only possible with a more resilient perovskite incorporated in a highly protective device design. [http://dx.doi.org/10.1063/1.4961210]

After merely four years since its realization as solid-state device,[1] the perovskite solar cell has achieved an efficiency of 22.1% exceeding even that of multicrystalline silicon.[2] That in itself is remarkable for a technology as new young as the perovskite cell. However, more impressive is the fact that the perovskite absorber can be processed simply from solution and/or vapor.[3–5] The fact that the efficiency is now on par with that of established photovoltaic technologies spurs the dreams of a rapid transition from a laboratory technology to an industrial-scale solar power technology. Without the complex material processing of its competitors and the abundance of its fundamental materials, the perovskite solar cell could thus provide even cheaper clean energy.

Simple processing comes at a price for the perovskite solar cell. Because the material is soluble in aprotic polar solvents, it degrades readily and quickly when it comes in contact with even small amounts of such solvents such as water.[6] The big challenge for the perovskite solar cell, which it needs to overcome in order to become a mature photovoltaic technology, is the aspect of stability so that it may have a chance to comply with the common standard for photovoltaic modules to retain their most of their initial efficiency for up to 25 years.[7]

In this Research Update, we will give a short and concise overview over the current efforts to enhance the stability and durability of perovskite solar cells. We can differentiate between two fundamental strategies: the first one is focused on the entire device seeking to guard and protect the absorber from external assaults by developing specialized functional barrier structures. The second strategy seeks to improve the resilience and stability of the absorber itself. This can be done by either altering the elemental composition of the perovskite or by modifying the perovskite absorber with functional molecules with the purpose of making the perovskite less susceptible to, for example, moisture degradation.

[a]habisreutinger@physics.ox.ac.uk

Various excellent reviews (see Seigo Ito *et al.* in this issue) give an extensive overview over the current understanding of the weaknesses of the most common perovskite absorbers and the most detrimental external forces.[6,8–10] We will therefore confine ourselves to a concise descriptive account of the most common degradation pathways in order to give context for the strategies to halt and prevent them.

In the very first attempts to integrate the perovskite absorber into photovoltaic devices, methylammonium lead triiodide ($MAPbI_3$) was used as sensitizer in liquid-state dye-sensitized solar cells.[11,12] The authors noted that the perovskite would degrade within minutes when in contact with acetonitrile and ethyl acetate, which were used as electrolyte, respectively. This observation already pointed towards the inherent vulnerability of the perovskite material to aprotic polar solvents. The most ubiquitous member of this class of solvents is water. In fact, the structural integrity of perovskite films was shown to be compromised by the presence of atmospheric moisture within a timeframe of a few hours.[13] The degradation mechanism has been documented and described in detail.[14–16] Essentially, because the organic methylammonium cation is only weakly bound via hydrogen bonds to the ionic cage of lead and iodide, a water molecule can break these bonds. As a consequence, the methylammonium is solubilized by water and afforded greater mobility to move throughout the structure. During the formation process of the perovskite, this can be beneficial by facilitating the removal of excess methylammonium.[17] Similarly, a limited exposure to moisture after complete crystallization can improve the optoelectronic properties of the perovskite.[17] However, the increased mobility of the solubilized methylammonium also destabilizes the material because external forces such as heat and light can lead to the removal of the volatile organic constituent, which results in the decomposition to lead iodide.[13] In the presence of external forcing, this decomposition process can be initiated by individual molecules of water.[16,18] This shows that the methylammonium based perovskite is highly sensitive to even minuscule amounts of water. An integral part of devices employing this perovskite absorber must therefore be a barrier to prevent moisture ingress.

Following the initial incarnation of the solid-state perovskite solar cell, the most common device architecture is still the n-i-p structure, in which electrons are collected by the transparent electrode at the bottom; while the top-layer is a hole-collecting layer extracting the holes. Being the top layer of the device, the hole-transporter can be considered the first line of defense against moisture ingress.

A variety of approaches has been explored to improve the moisture-blocking properties of this layer. A focal point of many studies has been the relatively poor barrier property of the most commonly employed hole-transporting materials, namely, spiro-OMeTAD, poly(triarylamine) (PTAA), and poly(3-hexylthiophene) (P3HT), to effectively prevent moisture ingress.[13] The combination of heat, light, and moisture generally results in rapid degradation of the perovskite layer underneath the hole-transporters, which occurs even more rapidly when the hole-transporting materials (HTMs) are doped with a hygroscopic dopant such as Li-TFSI.[13,14,19,20] Removing the need for such a dopant is an obvious strategy to improve the moisture resilience and overall device stability.[21–27] This can be achieved by replacing the reactive dopants with inert additives such as carbon nanotubes or graphene,[21,28] or by pre-oxidizing a fraction of the hole-transporter in order to improve the charge transport characteristics of the undoped hole-transporting material.[23,29] Nguyen *et al.* could show that by pre-oxidizing a small fraction of spiro-OMeTAD, the overall conductivity of the hole-transporter is increased significantly, yielding device performances comparable to devices with conventional Li-TFSI doping but more stable performance under illumination.[23] Leijtens *et al.* showed that the same technique of partial pre-oxidation can be used on a range of other small-molecule hole-transporters to improve their charge transport characteristics.[29] Removing the need for external dopants can also be achieved by synthesizing novel hole-transport materials which have tailored energy levels and inherently good charge transport characteristics and therefore do not require additional doping for efficient charge extraction.[22,24,25,27,30] Promising results were obtained by Kim *et al.*, employing a newly synthesized polymer as hole-transporter which was shown to protect the perovskite absorber for 1400 h at 75% relative humidity in the dark and at room temperature (Fig. 1(c)).[27] Unfortunately, the authors compare their dopant-free polymer to doped

spiro-OMeTAD on the basis of hysteretic current-voltage scans, failing to report the steady-state performance.[27]

To further boost the resilience against moisture ingress into the device, hydrophobicity has become an additional important aspect informing the synthesis of new hole-transporting materials. In fact, hole transporters specifically designed to have intrinsic hydrophobic properties are able to halt creeping moisture ingress and thus improve the device stability.[13,19,22,29,31,32] In our study, we developed a two-layer system composed of single-walled carbon nanotubes for selective charge extraction and an encapsulating polymer matrix such as poly(methyl methacrylate) or polycarbonate to protect the device from moisture ingress.[13] The devices remained stable in ambient humidity conditions at elevated temperatures of 80 °C, while control devices were shown to rapidly degrade (Figs. 1(a) and 1(b)).[13] The protective effect of the encapsulating polymer even allowed the direct exposure to running water for a short amount of time.

Leijtens *et al.* demonstrated that their hydrophobic hole-transporter can be resilient under even harsher stability tests such as full water immersion.[29]

Moisture penetration of the hole-transporting layer can also be achieved by crosslinking the hole-transporter to thusly minimize the moisture ingress pathways.[26] Xu and co-workers synthesized an arylamine derivative (*N*4,*N*4′-Di(naphthalen-1-yl)-*N*4,*N*4′-bis(4-vinylphenyl)biphenyl-4,4′-diamine) (VNBP) which can be thermally crosslinked.[26] A thin layer of MoO_3 deposited on top p-dopes the polymer without compromising its barrier function, and allowing it to achieve a steady-state efficiency of 16.5%.[26] Even more impressively, the VNBP-MoO_3 double layer protects the perovskite absorber from degradation and retains its high performance under harsh stressing conditions. Devices were shown to withstand thermal stressing at 110 °C for 1 h (Fig. 1(d)) and high humidity exposure at 70% relative humidity for 30 days. This resilience against degradation can probably be credited to the excellent barrier properties of the crosslinked double-layer hole-transporting layer preventing moisture ingress and methylammonium egress. This is illustrated by the fact that devices remained unaffected even when being exposed to both polar and non-polar solvents.[26] The resilience against solvents may in particular hold a lot of promise for tandem applications.

One of the most compelling long-term testing regimes has been reported by Abate *et al.* who were investigating silolothiophene-linked triphenylamines as hole-transporters.[33] Using maximum power-point tracking, the steady-state performance of devices with one of the doped triphenylamine hole-transporters and doped spiro-OMeTAD was continuously measured under ultraviolet (UV)-filtered simulated sunlight in an argon atmosphere at around 45 °C for up to 1000 h.[33] By fitting a double-exponential decay to the power-output of the devices, the authors could extract a half-life for the two compared materials. The triphenylamine outperformed spiro-OMeTAD with a half-life of 6000 h, compared to 1000 h, which the authors attribute to a better thermal stability.[33] Further studies of this sort will be very insightful with respect to the device stability, in particular, if they were to include relevant stressors such as moisture, oxygen, and UV light. A range of inorganic hole-transporter materials were proposed with the aim of improving the device stability, including copper thiocyanate (CuSCN),[34–41] copper iodide (CuI),[42,43] and nickel oxide (NiO_x).[44] The latter for example showed good stability over 60 days, during which control devices with spiro-OMeTAD underwent rapid degradation.[44]

Evidently, next to high power-conversion efficiencies and a simple synthesis, the aspect of stability has become an important benchmark for new hole-transporter systems.[45] In numerous publications, beneficial properties of hole-transporter have been claimed; however, a majority of those studies relies on "cupboard aging" or "shelf-live assessment," where devices are stored in a dark and often dry environment, and tested at different time points. It is worth pointing out that this kind of "aging" is insufficient to assess the overall stability of functional devices, in general, and the protective effect of the hole-transporter, in particular, because the driving forces of the absorber degradation have largely been removed.[6] In order to provide unassailable evidence for improved device stability, devices should remain operational for an extended period of time being exposed to either full solar spectrum illumination, an increased temperature around 85 °C, an external load equivalent to maximum power-point operation, or a combination thereof.

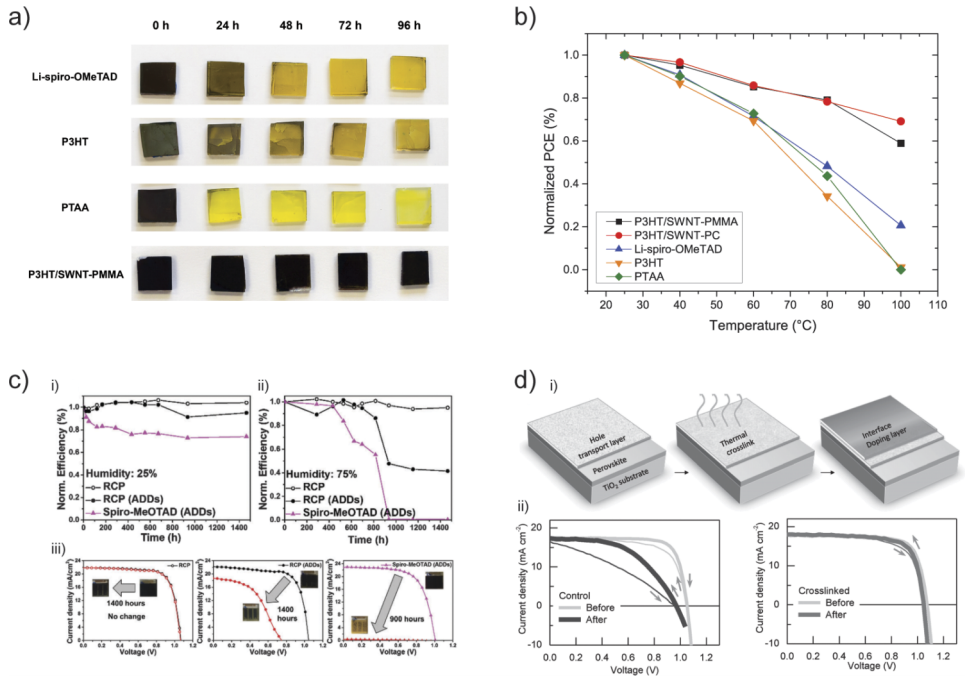

FIG. 1. (a) shows photos illustrating the time evolution of $MAPbI_3$ films with different hole-transporting layers exposed to 80 °C under ambient conditions. The conversion from the dark initial color to yellow indicates the degradation of the perovskite material to lead iodide. Over 96 h of heat exposure, only a composite structure of carbon nanotubes and PMMA was able to prevent degradation. This also translates to better operational stability at elevated temperatures as shown in (b) [reproduced with permission from Habisreutinger *et al.*, Nano Lett. **14**, 5561 (2014). Copyright 2014 American Chemical Society]. (c) Stability data for devices with a dopant-free hole-transporter. It shows the superior stability of the dopant-free material at 25% humidity in (i) and at 75% humidity in (ii). In (iii) the evolution of the current-voltage scans over time is shown [reproduced with permission from Kim *et al.* Energy Environ. Sci., **9**, 2326 (2016). Copyright 2016 The Royal Society of Chemistry]. (d) (i) shows the crosslinked MoO_x-doped hole-transport system described by Xu *et al.*[26] In (ii) the effect of a 60 min burn-in stress test at 110 °C on the JV-curves of a spiro-OMeTAD control and the crosslinked HTM is shown [reproduced with permission from Xu *et al.*, Adv. Mater. **28**, 440 (2016). Copyright 2016 Wiley-VCH Verlag GmbH & Co. KGaA].

Stability is clearly moving more and more into the focus of the development of new hole-transporters for perovskite solar cell; however, to-date, the highest efficiencies are still obtained using the established hole-transporter materials spiro-OMeTAD and PTAA.[5,46,47] Both these hole-transporters have been shown to lack the ability to effectively block moisture ingress.[13] However, there is another strategy that seeks to enhance the device stability against moisture for these materials, by introducing a very thin layer of an insulating water-impermeable material between the perovskite absorber and the hole-transporter. Several such barrier materials have been explored and shown to reduce moisture ingress and improve stability in a non-dry environment.[48–52] Using atomic layer deposition (ALD) as a technique to deposit an ultrathin layer of Al_2O_3 between the perovskite and spiro-OMeTAD, the stability of a device kept at RH 50% without illumination for 24 days could be improved and its performance was reported to still be at 90% of the initial value.[48] Guarnera *et al.* showed that a simply spin-coated layer of alumina nanoparticles at the interface of the perovskite absorber and spiro-OMeTAD improves performance and stability.[49] A sealed device with the buffer layer experienced a performance decrease of merely 5% over 350 h of continuous full-spectral illumination at AM 1.5. The performance of a control device without the buffer dropped to around 40% of its initial efficiency within the same time frame.[49]

Several hydrophobic organic layers have been employed at the interface between the $MAPbI_3$ perovskite and spiro-OMeTAD to act as moisture barriers. The layers have to be thin enough to allow charge transfer but thick enough to effectively block moisture ingress. Pentafluorobenzenethiol, for example, was shown to increase the device durability at a relative humidity of

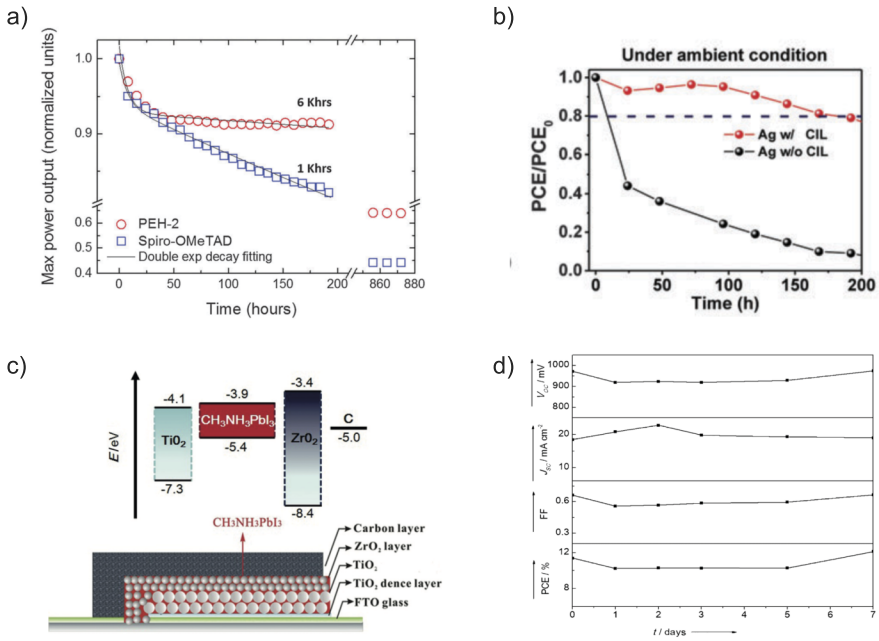

FIG. 2. (a) Abate and co-worker's stability data, showing the superior long-term stability of devices with a silolothiophene-linked triphenylamine as hole-transporters under stressor-free conditions [reproduced with permission from Abate *et al.*, Energy Environ. Sci., **8**, 2946 (2015). Copyright 2016 The Royal Society of Chemistry]. (b) Neutralizing ionic defects is shown by Back *et al.* to significantly enhance the long-term performance of p-i-n device, determined by current-voltage sweeps in a nitrogen atmosphere. The inset shows the device performance, as a function of maximum power-point tracking under N_2 [reproduced with permission from Back *et al.*, Energy Environ. Sci. **9**, 1258 (2016). Copyright 2015 The Royal Society of Chemistry]. (c) Architecture and energy scheme of mesoscopic perovskite cell in which the carbon electrode provides significant air stability. This stability is demonstrated in (d) which shows the time evolution of the performance parameters of such a device with encapsulation during outdoor aging in Jeddah, Saudi Arabia [reproduced with permission from Li *et al.*, Energy Technol. **3**, 551 (2015). Copyright 2015 Wiley-VCH Verlag GmbH & Co. KGaA].

45%.[53] Modifying the perovskite surface with dodecyltrimethoxysilane (C_{12}-silane), the devices lost merely 15% of their initial efficiency after 600 h under ambient conditions.[54]

The main objective of many barrier layers is to hamper any moisture diffusion through the hole-transporter to prevent degradation. However, several studies have shown that another source for device impairment is chemical reactions between the iodide ions from the perovskite and the metal electrode, typically Ag or Al.[55–58]

This can result in the formation of an insulating barrier such as Ag-ı which will impair charge extraction at this electrode.[59] Long-term operability of these devices requires therefore, that, additionally to moisture ingress from the outside, the diffusion of ions from the perovskite to the electrode is blocked in order to avoid electrode corrosion. Sanehira and co-workers found that this degradation pathway can be blocked for aluminum by inserting a thin layer of MoO_x between the spiro-OMeTAD layer and the metal electrode.[50]

Back *et al.* approached this issue by focusing on chemically stabilizing the ionic defects thought to be responsible for the iodization of the electrode by introducing a chemical inhibition layer at the interface with the metal electrode (Fig. 2(b)).[55]

Greater electrode stability could also be achieved by Guerrero *et al.* by moving away from using either Ag or Al, and instead employing a Cr_2O_3/Cr electrode which is shown to be chemically inert towards iodide.[58] Similarly, Au electrodes do not undergo any corrosion; however, the price of the metal is prohibitively high for large-scale commercialization. Ku *et al.* have pioneered a very promising approach of employing a thick carbon electrode.[60] The carbon cathode is inexpensive, is not prone to corrosion, and, interestingly, can act as hydrophobic moisture barrier additionally increasing the stability of a perovskite solar cell.[60–64] In some architectures, devices using the carbon cathode do not even require a selective p-type contact.[60–62,65,66] Most remarkable is a

triple-layer structure composed of mesoporous TiO_2 and mesoporous ZrO_2, which is then infiltrated with $MAPbI_3$ and contacted by a thick carbon layer.[61] In the initial report, stable performance under full sunlight illumination, unencapsulated in ambient air for a period of more than 1000 h was reported.[61] The stability of this architecture has been further demonstrated since with a range of stress-tests including outdoor testing (Figs. 2(c) and 2(d)).[66] An encapsulated device was reported to show a remarkably stable performance when aged outdoors for seven consecutive days in Jeddah, Saudi Arabia. Further, the performance was also reported to remain stable when an encapsulated device was thermally stress-tested by keeping it 80-85 °C for 90 days, in the dark. Photostability of the perovskite devices was also demonstrated by continuously monitoring the power-output of an unencapsulated device in an argon atmosphere at 45 °C and at maximum power-point tracking conditions. However, not the full sunlight spectrum was used in this experiment, instead an light-emitting diode (LED) array served as light source, emitting only in the visible range without including contributions from the UV region. In light of previous studies observing photo-induced degradation of perovskite devices due to the photoactivity of mesoporous TiO_2 for the UV range,[67] a more rigorous photostability study with a full AM 1.5 spectrum matching the spectral range of natural sunlight is therefore needed in order to obtain a complete picture of the "real-world" stability of this architecture.

The device performances of p–i–n perovskite solar cells using CIL/Ag and Ag electrodes, as a function of the J–V sweep operation time under N_2 (Fig. 2(b)). The inset also represents the device performance, as a function of MPP tracking time under N_2.

The discussed strategies to improve the device stability thus far have been mainly targeted at the inherent vulnerability of $MAPbI_3$ to moisture and the subsequent degradation of the absorber. As discussed before, being a highly polar solvent, water has the ability to solubilize the organic constituent of the perovskite, thusly compromising the structural integrity and stability of the material, in particular, in the presence of exterior stressors. The stability of perovskite devices can therefore be significantly improved by preventing or minimizing the ingress of moisture.

However, there is mounting evidence that oxygen also induces rapid perovskite degradation.[6,67–71] Ambient oxygen in combination with light can lead to direct photo-oxidation of the $MAPbI_3$ perovskite.[68,69] Those studies suggest that the accumulation of photogenerated electrons accelerates the oxygen-induced degradation of the perovskite absorber. Possible strategies for mitigating the oxygen assault on devices could therefore include effective barrier layers and oxygen-impermeable encapsulants, as well as efficient electron extraction layers. Several studies have reported improved device stability when mesoporous layers of TiO_2 particles or nanorods are employed as rapid electron extraction pathways.[70,72–74]

This strategy has to take into account, however, that metal-oxides such as TiO_2 are themselves photoactive materials for UV-induced redox reactions.[75–77] In their study, Leijtens and co-workers investigated the impact of UV-irradiation on perovskite devices on mesoporous TiO_2, observing that photoinduced oxygen desorption over time generates shallow traps below the conduction band edge thus resulting in decreased performance.[67]

C_{60} was used by Wojciechowski as interface modification layer for TiO_2 and as stand-alone electron-accepting layer.[78,79] The latter was shown to yield a more stable device performance under full-spectrum illumination for 500 h, whereas the control device with TiO_2 as n-type layer experienced a significant reduction in performance.[79] Ito *et al.* employed a buffer layer of Sb_2S_3 between TiO_2 and the perovskite, thus significantly improving the device stability under light exposure.[34] The protective effect of Sb_2S_3 is credited to the ability of the inorganic layer to block the photocatalytic decomposition of the perovskite at the interface with TiO_2, which is a well-known photocatalyst.[76,77] The control devices, in which the perovskite was coated directly onto TiO_2, were shown to degrade rapidly which the authors attribute to a UV-induced photo-oxidation process at the TiO_2 surface.[34] This vulnerability to UV-activated degradation processes at the TiO_2 interface was confirmed by Li *et al.*[80] In this study, the authors were able to stabilize the perovskite absorber by inserting a thin layer of CsBr between TiO_2 and the perovskite, thus inhibiting the photocatalytic decomposition of the absorber.[80] Another strategy to impede performance losses due to photoactivated absorber degradation was demonstrated by Pathak *et al.*, who doped the mesoporous TiO_2

layer with aluminum.[81] Devices with the Al-doped TiO_2 layer exhibited a much enhanced operational stability under full illumination in an inert atmosphere. The increase in stability was attributed to the substitutional incorporation of Al in the anatase lattice, thus passivating UV-generated oxygen vacancies acting as electronic trap sites on the TiO_2 surface.[81] While Al-doping makes the devices more stable, it also causes the conduction band edge of TiO_2 to shift upwards, which negatively impacts the charge extraction efficiency and results in a reduced photocurrent. This drawback can be overcome by using neodymium (Nd) instead of Al as dopant, leaving the conduction band position of TiO_2 unchanged. Devices with a Nd-doped mesoporous TiO_2 layer were shown to reach a steady-state efficiency of up to 18.2% while exhibiting a significantly enhanced stability compared to their undoped counterparts.[82]

Hwang and co-workers went one step further by completely replacing TiO_2 with CdS as the n-type layer in order to improve the device photostability.[83] The authors report that after continuous illumination for 12 h, devices with TiO_2 as n-type layer experienced a significant decrease in efficiency from 15.4% to 3.1% whereas the devices with CdS had retained more than 90% of their initial efficiency.[83]

The devices discussed thus far had the same n-i-p architecture, in which the device stack is configured such that electrons are extracted at the bottom by an n-type layer, and the transparent electrode, whereas holes are extracted at the top by a p-type layer and an opaque electrode. In this configuration, moisture ingress through the p-type conductor and photo-oxidation on the n-type interface cause degradation.

Conversely, this architecture can also be inverted to form a p-i-n structure. The n-type contact is typically formed by phenyl-C_{61}-butyric acid methyl ester (PCBM) while the most commonly used transparent hole-selective contact is poly(3,4-ethylenedioxythiophene) poly(styrenesulphonate) (PEDOT:PSS).[84,85] The biggest stability concern is the acidic and hygroscopic nature of PEDOT:PSS which may lead to degradation of the perovskite absorber at the interface.[86] To prevent direct contact between the corrosive PEDOT:PSS and the transparent electrode, thin inorganic blocking layers were proposed.[87,88] Such bilayer structures of PEDOT:PSS and the buffer layer were reported to experience less of a performance decrease than pristine PEDOT:PSS.[87,88] The thin interlayer of $CuAlO_2$ and MoO_3 are credited, respectively, with suppressing corrosion of the transparent indium-tin oxide (ITO) electrode by the acidic PEDOT:PSS.[87,88] In a similar vein, to mitigate this electrode corrosion, GeO_2 was blended into the PEDOT:PSS dispersion prior to its deposition. The reasoning was that GeO_2 due to its alkaline nature in aqueous solutions may be able to buffer the acidity of PEDOT:PSS to mitigate any ITO corrosion. In devices the hybrid p-type layer showed a much more stable performance than pristine PEDOT:PSS but still dropped to mere 50% of the initial performance within 26 h.[89]

Thus far stabilizing devices with PEDOT:PSS as hole-extraction layer appears to be quite difficult with PEDOT:PSS attacking both of its interfaces. Choi and co-authors therefore abandoned PEDOT:PSS altogether and achieved a significant improvement in device stability in air by employing a pH-neutral polyelectrolyte.[86] Reduced graphene-oxide may also be a candidate as an inert and stable replacement for PEDOT:PSS.[90] However, while devices with RGO appear to be less prone to degradation when exposed to ambient air—as opposed to devices with PEDOT:PSS—the overall performance still decreased significantly within 140 h.[90] A material which holds a lot of promise as a stable hole-transport layer for devices with the p-i-n architecture is the inorganic NiO_x, which is known for its good environmental stability. Compared to PEDOT:PSS devices with copper-doped NiO_x exhibit in fact a significantly increased air stability, retaining around 90% of their initial efficiency after dark ageing for 240 h in ambient air, whereas PEDOT:PSS devices experienced a rapid decrease of more than 50% within 144 h.[91] Following up with a solution-processed approach to depositing NiO_x, Kim *et al.* showed this inorganic p-type layer can also be applied on flexible substrates yielding more air-stable flexible devices.[92]

In the inverted architecture, the top layer of the device is a thin n-type layer, typically PCBM.[84,93] With a thickness of merely tens of nanometers, it constitutes a poor barrier against water and oxygen penetration. In their study, You *et al.* therefore tackled the issue of instability for both charge-selective layers, namely, PEDOT:PSS and the PCBM, by replacing the two organic layers with inorganic ones, NiO_x on the p-side and ZnO on the n-side.[94] Kept in ambient air in the dark, the

TABLE I. Overview of literature values on long-term stability strategies, including relevant parameters such as relative humidity, atmosphere, illumination, and UV irradiation. The figures of merit are the initial power-conversion efficiency, the rate of decreasing efficiency (in %/100 h), the total decrease in efficiency, as well as the decline in efficiency of the respective control system.

Reference	System	Structure	Humidity (RH) (%)	Atmosphere	MPP	Light (mW cm^{-2})	UV	Heat (°C)	Time (h)	Initial PCE (%)	Decrease rate (%/100 h)	Total decrease (%)	Control degradation (%)
13	SWNT-PMMA	HTL	50	Air	…	…	…	80	96	15.3	0	0.0	100.0
19	PDPPDBTE	HTL	20	Air	…	…	…	…	1000	8.5	0	0.0	23.0
22	TTF-1	HTL	40	Air	…	…	…	…	500	10.0	4	20.0	60.0
25	DER3T-TBDT	HTL	0	N_2	…	…	…	…	220	15.0	0	0.0	…
26	VNPB-MoO_3	HTL	0	N_2	…	…	…	110	1	16.5	0	0.0	30.0
27	RCP	HTL	75	Air	…	…	…	…	1400	17.3	0	0.0	100.0
28	P3HT-GD	HTL	<20	Air	…	…	…	…	2520	13.2	…	9.0	…
30	HAT-CN	HTL	<20	Air	…	…	…	…	1000	7.1	1.25	12.5	…
31	DR3TBDTT + PDMS	HTL	<20	Air	…	…	…	…	312	8.3	0.64	2.0	6.0
32	SAF-OMe	HTL	30	Air	…	…	…	…	240	15.2	16.3	39.0	55.0
33	PEH-2	HTL	0	Argon	Yes	100	…	45	850	13.0	4.1	35.0	55.0
34	Sb_2S_3	HTL	…	Air	…	…	…	…	10.8	6.0	…	35.0	…
42	CuI	HTL	…	Air	…	100	Yes	…	2	5.0	…	0.0	10.0
43	CuI	HTL	…	Air	…	…	…	…	600	4.0	6.7	40.0	…
44	NiO_x	HTL	30	Air	…	…	…	…	1440	7.2	0	0.0	100.0
49	Al_2O_3	Interface modifier	…	Air	…	100	Yes	…	350	10.0	1.4	5.0	60.0
52	Al_2O_3	Interface modifier	60	Air	…	100	Yes	…	18	4.6	…	48.0	80.0
53	HS-PhF_5	Interface modifier	45	Air	…	100	Yes	…	4	11.2	…	64.0	100.0
54	C_{12}-silane	Interface modifier	45	Air	…	…	…	…	600	13.7	2.5	15.0	35.0
55	CIL	Interface modifier	0	N_2	Yes	100	Yes	…	12	16.1	…	20.0	80.0
60	Carbon	Electrode	…	Air	…	…	…	…	840	6.6	0	0.0	…
61	Carbon	Electrode	…	Air	…	100	Yes	…	1008	12.8	0	0.0	…
62	Carbon	Electrode	…	Air	…	…	…	…	2500	6.0	0	0.0	…

TABLE I. (*Continued.*)

Reference	System	Structure	Humidity (RH) (%)	Atmosphere	MPP	Light (mW cm^{-2})	UV	Heat (°C)	Time (h)	Initial PCE (%)	Decrease rate (%/100 h)	Total decrease (%)	Control degradation (%)
63	Carbon	Electrode	40	Air	…	…	…	60	1000	14.9	2	20.0	…
66	Carbon	Electrode	0	Argon	Yes	100	…	45	1056	8.2	0	0.0	…
72	$TiCl_4$-NR	ETL	<35	Air	…	…	…	…	1320	12.0	3	40.0	100.0
73	TiO_2-MOF	ETL	…	Air	…	…	…	…	720	6.4	0.04	0.3	…
74	ZnO-NR	ETL	…	Air	…	…	…	…	500	5.0	2.6	13.0	…
79	C_{60}	ETL	…	Air	Yes	81.1	Yes	60	500	10.4	10	50.0	60.0
80	CsBr	Interface modifier	…	Air	…	523	365 nm	…	0.33	14.7	…	30.0	100.0
81	TiO_2-Al	ETL	…	Encapsulated	…	…	…	…	35	13.8	…	66.0	100.0
82	TiO_2-Nd	ETL	…	Air	Yes	100	Yes	…	3	18.2	…	14.0	30.0
83	CdS	ETL	…	Air	…	100	Yes	…	12	12.2	…	9.0	82.0
86	CPE-K	HTL	…	Air	…	…	…	…	0.58	12.5	…	55.0	99.0
87	a:$CuAlO_2$	HTL	…	Air	…	…	…	…	240	14.5	7.1	17.0	65.0
89	PEDOT:PSS-GeO_2	HTL	…	Air	…	100	Yes	…	78	15.2	…	72.0	85.0
90	RGO	HTL	…	Air	…	…	…	…	140	9.5	27.1	38.0	100.0
91	Cu:NiO_x	HTL	…	Air	…	…	…	…	240	15.0	4.2	10.0	70.0
92	CuPc/Carbon	HTL + electrode	…	Air	…	…	…	…	600	16.1	1.4	8.5	100.0
94	NiO_x + ZnO	HTL + ETL	30-50	Air	…	…	…	…	1440	16.1	0.7	10.0	100.0
98	Teflon	Encapsulation	…	Air	…	…	…	…	720	11.8	0.8	6.0	44.0

device with the inorganic charge-transport layers retained most of its initial performance for up to 60 days.[94]

The outermost modification to enhance the stability of a perovskite solar cell is the encapsulation of a device. This strategy involves a material which is resilient against moisture and oxygen permeation, and which is used to fully encapsulate the device with strategic placements of the electrode strips which can still be accessed without compromising the integrity of the protective encapsulation. Much work on the effectiveness of various sealing techniques has been carried out in the field of organic solar cells, as oxygen-induced degradation is one of the major factors compromising the stability of organic solar cells. The most effective method is the encapsulation of the device with a glass or metal plate using a slow-permeation epoxy material as sealant.[95–97] This technique should be perfectly adequate for perovskite devices as long as they are fabricated on rigid substrates. Hwang *et al.* showed that they could also improve the performance lifetime of a device by spinning a layer of amorphous Teflon on top of the device.[98] Chang *et al.* use the concept of a dense alumina layer as protective barrier and show that the atomic layer deposition of an Al_2O_3 layer significantly improves the air-stability due to the very low oxygen and water vapor transmission of the barrier layer.[99] More challenging is the device encapsulation for devices on flexible substrates. Weerasinghe and co-workers show that full encapsulation is needed for a flexible device.[100] Employing a commercial plastic barrier film, stable performance can be achieved over a period of up to 500 h. In Table I, an overview is given of stability metrics reported in literature for various approaches to stabilize $CH_3NH_3PbI_3$.[100]

To date, the inherent instability of $MAPbX_3$ materials towards moisture, heat, and ultraviolet (UV) light in presence of oxygen has been reported.[6,69] As discussed, methylammonium-based PSC tends to hydrolyze in the presence of moisture, thus triggering a non-reversible degradation process.[52,101,102] Although it has been reported that intermediate monohydrate phases can revert back to $MAPbI_3$, further degradation results in a final decomposition products of PbI_2 and aqueous CH_3NH_3I, which further decompose into volatile compounds such as CH_3NH_2, HI, or I_2.[14–16,52,103,104] Similarly, $HC(NH_2)_2PbI_3$ decomposes to $HC(NH_2)_2I$ and HI, where $HC(NH_2)_2I$ further decomposes to the volatile sym-triazine and NH_4I.[105,106] Moreover, it has been reported that $MAPbI_3$ also structurally degrades in an inert N_2 atmosphere when bulk powders and single crystals heated at temperature in excess of 200 °C,[107,108] while thin film can show signs of degradation at temperatures of 85 °C.[109] Here, we discuss recent advances in improving the inherent instability of the photoactive absorber material used in photovoltaic devices by tuning the perovskite composition.

A proposed route for stability improvement focused on the tuning of the ABX_3 general structure, where A is a cation, B is a divalent metal ion, and X is a halide. Seok and co-workers have reported on an improved stability to moisture when by controlling the halide composition.[110] By partially replacing the iodide with a bromide anion for the $MAPbX_3$ perovskite system, the authors were able to form a cubic three-dimensional (3D) perovskite structure phase of the $Pm\bar{3}m$ space group, instead tetragonal I4/mcm space group. This phase transition results in a slight rotation of the PbX_6 octahedrons, thus reducing the octahedra tilting and lattice distortion.[110]

Tuning of the X halide composition, in the general ABX_3 formula, can also be achieved via incorporation of an entire functional group, notably thiocyanate (SCN) group. Due to its similar ionic radius of 0.215–0.220 nm for SCN^- compared to 0.22nm for I^-, this pseudohalogen can replace a "true halide" such as the I^- halogen ion.[111,112] The partial halide substitution, forming a $MAPbI_{3-x}(SCN)_x$ perovskite structure, have had a beneficial impact on grain sizes and trap density,[111] optoelectronic properties,[113] and most importantly on its material stability.[114–116] In the case of $MAPb(SCN)_2I$, the interaction between Pb^{2+} and SCN^- is much stronger than in the case of neat $MAPbI_3$.[114] This stronger interaction suppresses the initial degradation mechanism involving the formation of hydrated intermediate containing isolated PbI_6^{4-} octahedral.[14] Jiang *et al.* reported that $MAPb(SCN)_2I$ decomposed at a significantly slower rate than $MAPbI_3$ when exposed to a 95% RH atmosphere.[114] Furthermore, a later study demonstrated that the $MAPbI_{3-x}(SCN)_x$ perovskite, fabricated via a two-step sequential deposition in a humid atmosphere using a $Pb(SCN)_2$ precursor instead of the conventional PbI_2 route, produced higher solar cell performance.[116] The

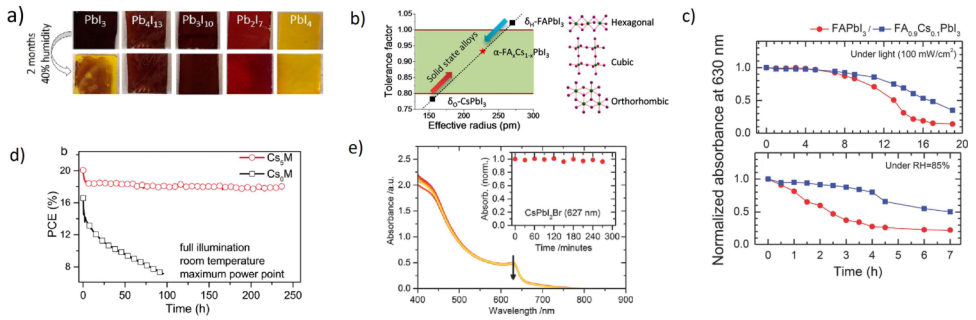

FIG. 3. (a) Images of five different perovskite films before and after exposure to humidity [reproduced with permission from Cao *et al.*, J. Am. Chem. Soc. **137**, 7843 (2015). Copyright 2015 American Chemical Society]. (b) Correlations between tolerance factor and crystal structure of perovskite materials [reproduced with permission from Li *et al.*, Chem. Mater. **28**, 284 (2015). Copyright 2015 American Chemical Society]. (c) Normalized absorbance of $FAPbI_3$ and $FA_{0.9}Cs_{0.1}PbI_3$ films measured under sulfur lamp (relative humidity (RH) < 50%, temperature (T) < 65 °C) and under constant humidity of RH 85% in dark (T = 25 °C) as a function of time [reproduced with permission from Lee *et al.*, Adv. Energy Mater. **5**, 1501310 (2015). Copyright 2015 Wiley-VCH Verlag GmbH & Co. KGaA]. (d) Aging for 250 h of $Cs_{0.05}(MA_{0.17}FA_{0.83})_{(0.95)}Pb(I_{0.83}Br_{0.17})_3$ and $MA_{0.17}FA_{0.83}Pb(I_{0.83}Br_{0.17})_3$ devices in a nitrogen atmosphere held at room temperature under constant white illumination and maximum power point tracking [reproduced with permission from Saliba *et al.*, Energy Environ. Sci. **9**, 1989 (2016). Copyright 2016 The Royal Society of Chemistry]. (e) Absorbance spectra for films of $CsPbI_2Br$ for different times of heating at 85 °C in 20%–25% RH [reproduced with permission from Sutton *et al.*, Adv. Energy Mater. **6**, 1502458 (2016). Copyright 2016 Wiley-VCH Verlag GmbH & Co. KGaA].

$MAPbI_{3-x}(SCN)_x$ solar cells without encapsulation retained 86.7% of the initial average efficiency, when stored in a 70% RH atmosphere for over 500 h, while $MAPbI_3$ lost nearly 40% of its original efficiency for an identical aging condition. Interestingly, it has also reported been reported that $Pb(SCN)_2$ can also be used to form a two-dimensional (2D) perovskite material: $(CH_3NH_3)_2Pb(SCN)_2I_2$.[115,117]

Two-dimensional structures with generic structural formula $(A)_2(CH_3NH_3)_{n-1}M_nX_{3n+1}$, where n is an integer, have been reported to have improved the perovskite's moisture stability due to its hydrophobic nature (Figure 3(a)).[118,119] By partially replacing the small MA^+ cation with a long-chain organic cations such as *n*-butylammine (BA) or $C_6H_5(CH_2)_2NH_3$ (PEA), the perovskite can form in a multilayered compound.[118,119] However, these homologous 2D materials have less ideal properties for solar cell applications due to a wider optical band gap. This may limit their use for tandem solar cell or luminescent applications.

A recently proposed route for stability improvement focuses on the tuning of the methylammonium A cation. Cation mixtures have been reported in the early stages of the emergence of PCS; for example, Pellet *et al.* introduced FA into the $MAPbI_3$ to extend the absorption onset, while Jeon *et al.* incorporated $MAPbBr_3$ into the $FAPbI_3$ structure to enhance its crystallinity and structural stability, thus improving its power conversion efficiency.[120,121] However recently, cation mixtures have gained attention as a means to increase the absorber material's resistance to moisture and heat degradation. These stability gains were achieved by substituting MA with formamidinium (FA),[122] cesium (Cs) cations,[123–126] or a mixture of the two (Figure 3(b) and 3(d)).[5,127–131] Eperon *et al.* reported that degradation was considerably slowed for $FAPbI_3$ compared to $MAPbI_3$ when heated at 150 °C.[122] Moreover, $MAPbI_3$ perovskite undergoes a reversible phase transition from tetragonal to cubic when heated above ~54–57 °C.[107] This change in symmetry, occurring within the operating temperature range of the solar cell, can potentially lead to an accelerated degradation of methylammonium-based cells when operated in real-life operating conditions. On the other hand, Lee *et al.* report that $FAPbI_3$ shows no phase transition in the range from 25 °C to 150 °C, thus eliminating significant lattice shrinkage during standard operating temperature range.[132] Although the $MAPbI_3$ perovskite has received significant research attention, the PSC field may ultimately choose to move away from this perovskite structure due to its inherently thermally unstable nature.

In spite of several advantages of $FAPbI_3$ over $MAPbI_3$, including having a narrower band gap and higher thermal stability, $FAPbI_3$ PSC have had limited success. This is partly due to the structural instability of the black trigonal (P3m1) perovskite polymorph in the presence of moisture,

resulting in a phase transition to a yellow hexagonal non-perovskite (P63mc) polymorph.[133] Stabilization of the black perovskite phase was achieved by substituting FAI for MAI or MABr, resulting in $FA_{1-x}MA_xPbI_3$ or $FA_{1-x}MA_xPbI_{3-y}Br_y$ perovskite compositions.[120,121] According to Binek *et al.* the stabilization of the 3D black FA-based perovskite, achieved with the incorporation of a smaller MA cation compared to FA, can be attributed to the larger dipole moment of MA, which arranges the PbI_6 octahedra with a pseudocubic symmetry via I-H hydrogen bonding or the increase in Coulomb interactions within the structure.[131] As a result, films remained stable and did not undergo any phase transition in the 25–250 °C temperature range.[131] However, the relatively volatile nature of the MA cation may still remain problematic for long-term stability.

Several research groups have recently reported on the incorporation of an inorganic A-site cation in the perovskite structure, notably cesium. Fully inorganic cesium-based perovskite has gained interest due to their potential of withstanding high temperatures.[123–126] $CsPbI_3$ forms in a cubic ($pm\bar{3}m$) perovskite structure with a band gap of 1.73 eV.[122,123] Unfortunately, $CsPbI_3$ is highly unstable in this crystal structure when exposed to air and quickly undergoes a reversible phase transition to a yellow orthorhombic phase material, unsuitable for solar cell applications. On the other hand, $CsPbBr_3$ is less susceptible to moisture compared to their iodide counterpart.[125,134] Although they show comparable power-conversion efficiency (PCE) to that obtained by $MAPbBr_3$, its wide optical bandgap of ~2.25–2.36 eV is not ideal for single-junction solar cell applications.[125,135] Several groups have suggested a compromise between neat iodide and neat bromide perovskite by employing a $CsPbI_2Br$ composition.[124,126,136] This mixed-halide composition offers a greater resistance to moisture than the neat iodide composition, while utilizing a narrower band gap than the neat bromide perovskite (Figure 3(e)).

Although purely inorganic $CsPbX_3$ perovskites have exhibited outstanding thermal stability, to date, their reported efficiencies have yet to compete with their organic counterpart. Nevertheless, it has been shown that the cesium cation can also be used to stabilize the $FAPbI_3$ crystal structure, instead of relying on relatively volatile MA cation.[128,129] Lee *et al.* reported that cesium not only increases the PCE via stabilization of black $FAPbI_3$ perovskite phase but also improves film stability against light and humidity. Pristine un-encapsulated $FAPbI_3$ devices showed 81% degradation after 30 min of white light illumination (100 mW cm^{-2}) in an ambient condition (RH < 40%), whereas $FA_{0.9}Cs_{0.1}PbI_3$ devices degraded by 67% for an identical time period (Figure 3(c)).[128] A subsequent study found that the shelf-life stability of $FA_{0.85}Cs_{0.15}PbI_3$ solar cells was greatly extended compared to neat $FAPbI_3$. The $FA_{0.85}Cs_{0.15}PbI_3$ devices showed no loss in their PCE when stored in the dark for 15 days in a 15% RH atmosphere.[129] Further reports also included the use of a halide mixture in combination with the FA/Cs cation mixture, resulting in improvements in crystallinity of the material.[127,130] Moreover, reports of adding a small amount of Cs to the $MA_{0.17}FA_{0.83}Pb(I_{0.83}Br_{0.17})_3$ structure, forming a "triple-cation," have shown enhancements in stability, reproducibility, and PCE.[5] Although the MA cation remained in the precursor solution, the triple-cation composition was able to maintain 90% of its original PCE, from 20% to 18% PCE, after 250 h of aging under solar illumination using a maximum power point tracking (MPPT), in an N_2 atmosphere.

Perovskite solar cells have achieved efficiencies which are already on par with inorganic thin-film technologies; the focus will therefore need to shift towards improving their long-term stability. The inherent instability of $MAPbI_3$ towards moisture and oxygen can be combatted by introducing functional barrier layers into the device structures, which allow efficient charge extraction while minimizing the ingress of degradation agents. This has been shown to improve device stability to some degree in the short run. But in many cases, this appears to delay rather than to prevent the absorber degradation. The second strategy stabilizes the perovskite absorber itself by substituting its constituent ions. Mixed cation and mixed halide compositions, as well as lower-dimensional structures, show very promising results. In essence, the weak point of the perovskite is the A-site cation, of which methylammonium is simply too volatile to be retained in the perovskite structure when exposed to external stressors; in contrast, the two alternatives, formamidinium and cesium, give the perovskite much better stability, but can only be stabilized in the right phase when present as ionic mixtures. While these optimized compositions improve the stability of the perovskite, they will still require highly resilient charge-selective layers, either inorganic or inert organic layers, and

mature encapsulation techniques in order to survive true long-term stability studies and systematic stress tests such as high-humidity and full-temperature cycles, which will be an important gauge for the maturity of this photovoltaic technology vis-à-vis its inorganic thin-film competitors.

This work was supported by the International Collaborative Energy Technology R&D Program of the Korean Institute of Energy Technology Evaluation and Planning (KETEP) with financial resource from the Ministry of Trade, Industry & Energy, Republic of Korea (No. 20148520011250), and by the Engineering and Physical Sciences Research Council (Grant No. EP/M023532/1) and the U.S. Office of Naval Research.

[1] M. M. Lee, J. Teuscher, T. Miyasaka, T. N. Murakami, and H. J. Snaith, Science **338**, 643 (2012).
[2] National Renewable Energy Laboratory, NREL Efficiency Chart, can be found under http://www.nrel.gov/ncpv/images/efficiency_chart.jpg, 2016.
[3] M. Liu, M. B. Johnston, and H. J. Snaith, Nature **501**, 395 (2013).
[4] J. Burschka, N. Pellet, S.-J. Moon, R. Humphry-Baker, P. Gao, M. K. Nazeeruddin, and M. Grätzel, Nature **499**, 316 (2013).
[5] M. Saliba, T. Matsui, J.-Y. Seo, K. Domanski, J.-P. Correa-Baena, M. K. Nazeeruddin, S. M. Zakeeruddin, W. Tress, A. Abate, A. Hagfeldt, and M. Grätzel, Energy Environ. Sci. **9**, 1989 (2016).
[6] T. Leijtens, G. E. Eperon, N. K. Noel, S. N. Habisreutinger, A. Petrozza, and H. J. Snaith, Adv. Energy Mater. **5**, 1500963 (2015).
[7] Z. Campeau, M. Mikofski, E. Hasselbrink, Y.-C. Shen, D. Kavulak, A. Terao, R. Lacerda, W. Caldwell, M. Anderson, Z. Defreitas, D. Degraaff, A. Budiman, and L. Leonard, *SunPower Module Degradation Rate* (SunPower Corporation, 2013).
[8] T. A. Berhe, W.-N. Su, C.-H. Chen, C.-J. Pan, J.-H. Cheng, H.-M. Chen, M.-C. Tsai, L.-Y. Chen, A. A. Dubale, and B.-J. Hwang, Energy Environ. Sci. **9**, 323 (2016).
[9] D. Wang, M. Wright, N. K. Elumalai, and A. Uddin, Sol. Energy Mater. Sol. Cells **147**, 255 (2016).
[10] B. Li, Y. Li, C. Zheng, D. Gao, and W. Huang, RSC Adv. **6**, 38079 (2016).
[11] A. Kojima, K. Teshima, Y. Shirai, and T. Miyasaka, J. Am. Chem. Soc. **131**, 6050 (2009).
[12] J.-H. Im, C.-R. Lee, J.-W. Lee, S.-W. Park, and N.-G. Park, Nanoscale **3**, 4088 (2011).
[13] S. N. Habisreutinger, T. Leijtens, G. E. Eperon, S. D. Stranks, R. J. Nicholas, and H. J. Snaith, Nano Lett. **14**, 5561 (2014).
[14] J. Yang, B. D. Siempelkamp, D. Liu, and T. L. Kelly, ACS Nano **9**, 1955 (2015).
[15] J. A. Christians, P. A. Miranda Herrera, and P. V. Kamat, J. Am. Chem. Soc. **137**, 1530 (2015).
[16] A. M. A. Leguy, Y. Hu, M. Campoy-Quiles, M. I. Alonso, O. J. Weber, P. Azarhoosh, M. van Schilfgaarde, M. T. Weller, T. Bein, J. Nelson, P. Docampo, and P. R. F. Barnes, Chem. Mater. **27**, 3397 (2015).
[17] G. E. Eperon, S. N. Habisreutinger, T. Leijtens, B. J. Bruijnaers, J. J. van Franeker, D. W. DeQuilettes, S. Pathak, R. J. Sutton, G. Grancini, D. S. Ginger, R. A. J. Janssen, A. Petrozza, and H. J. Snaith, ACS Nano **9**, 9380 (2015).
[18] J. M. Frost, K. T. Butler, F. Brivio, C. H. Hendon, M. van Schilfgaarde, and A. Walsh, Nano Lett. **14**, 2584 (2014).
[19] Y. S. Kwon, J. Lim, H.-J. Yun, Y.-H. Kim, and T. Park, Energy Environ. Sci. **7**, 1454 (2014).
[20] J. Liu, S. Pathak, T. Stergiopoulos, T. Leijtens, K. Wojciechowski, S. Schumann, N. Kausch-Busies, and H. J. Snaith, J. Phys. Chem. Lett. **6**, 1666 (2015).
[21] S. N. Habisreutinger, T. Leijtens, G. E. Eperon, S. D. Stranks, R. J. Nicholas, and H. J. Snaith, J. Phys. Chem. Lett. **5**, 4207 (2014).
[22] J. Liu, Y. Wu, C. Qin, X. Yang, T. Yasuda, A. Islam, K. Zhang, W. Peng, W. Chen, and L. Han, Energy Environ. Sci. **7**, 2963 (2014).
[23] W. H. Nguyen, C. D. Bailie, E. L. Unger, and M. D. McGehee, J. Am. Chem. Soc. **136**, 10996 (2014).
[24] Y. Liu, Q. Chen, H.-S. Duan, H. Zhou, Y. Yang, H. Chen, S. Luo, T.-B. Song, L. Dou, Z. Hong, and Y. Yang, J. Mater. Chem. A **3**, 11940 (2015).
[25] Y. Liu, Z. Hong, Q. Chen, H. Chen, W.-H. Chang, Y. M. Yang, T.-B. Song, and Y. Yang, Adv. Mater. **28**, 440 (2016).
[26] J. Xu, O. Voznyy, R. Comin, X. Gong, G. Walters, M. Liu, P. Kanjanaboos, X. Lan, and E. H. Sargent, Adv. Mater. **28**, 2807 (2016).
[27] G.-W. Kim, G. Kang, J. Kim, G.-Y. Lee, H. Il Kim, L. Pyeon, J. Lee, and T. Park, Energy Environ. Sci. **9**, 2326 (2016).
[28] J. Xiao, J. Shi, H. Liu, Y. Xu, S. Lv, Y. Luo, D. Li, Q. Meng, and Y. Li, Adv. Energy Mater. **5**, 1401943 (2015).
[29] T. Leijtens, T. Giovenzana, S. N. Habisreutinger, J. S. Tinkham, N. K. Noel, B. A. Kamino, G. Sadoughi, A. Sellinger, and H. J. Snaith, ACS Appl. Mater. Interfaces **8**, 5981 (2016).
[30] Y. Ma, Y.-H. Chung, L. Zheng, D. Zhang, X. Yu, L. Xiao, Z. Chen, S. Wang, B. Qu, Q. Gong, and D. Zou, ACS Appl. Mater. Interfaces **7**, 6406 (2015).
[31] L. Zheng, Y.-H. Chung, Y. Ma, L. Zhang, L. Xiao, Z. Chen, S. Wang, B. Qu, and Q. Gong, Chem. Commun. **50**, 11196 (2014).
[32] Y.-K. Wang, Z.-C. Yuan, G.-Z. Shi, Y.-X. Li, Q. Li, F. Hui, B.-Q. Sun, Z.-Q. Jiang, and L.-S. Liao, Adv. Funct. Mater. **26**, 1375 (2016).
[33] A. Abate, S. Paek, F. Giordano, J. P. Correa Baena, M. Saliba, P. Gao, T. Matsui, J. Ko, S. M. Zakeeruddin, K. H. Dahmen, A. Hagfeldt, M. Grätzel, and M. K. Nazeeruddin, Energy Environ. Sci. **8**, 2946 (2015).
[34] S. Ito, S. Tanaka, K. Manabe, and H. Nishino, J. Phys. Chem. C **118**, 16995 (2014).
[35] P. Qin, S. Tanaka, S. Ito, N. Tetreault, K. Manabe, H. Nishino, M. K. Nazeeruddin, and M. Grätzel, Nat. Commun. **5**, 3384 (2014).
[36] S. Ito, S. Tanaka, H. Vahlman, H. Nishino, K. Manabe, and P. Lund, ChemPhysChem **15**, 1194 (2014).
[37] S. Chavhan, O. Miguel, H.-J. Grande, V. Gonzalez-Pedro, R. S. Sanchez, E. M. Barea, I. Mora-Sero, and R. Tena-Zaera, J. Mater. Chem. A **2**, 12754 (2014).
[38] G. Murugadoss, G. Mizuta, S. Tanaka, H. Nishino, T. Umeyama, H. Imahori, and S. Ito, APL Mater. **2**, 081511 (2014).

[39] S. Ito, S. Tanaka, and H. Nishino, Chem. Lett. **44**, 849 (2015).
[40] S. Ito, S. Tanaka, and H. Nishino, J. Phys. Chem. Lett. **6**, 881 (2015).
[41] Y. Ma, L. Zheng, Y.-H. Chung, S. Chu, L. Xiao, Z. Chen, S. Wang, B. Qu, Q. Gong, Z. Wu, and X. Hou, Chem. Commun. **50**, 12458 (2014).
[42] J. A. Christians, R. C. M. Fung, and P. V. Kamat, J. Am. Chem. Soc. **136**, 758 (2014).
[43] G. A. Sepalage, S. Meyer, A. Pascoe, A. D. Scully, F. Huang, U. Bach, Y.-B. Cheng, and L. Spiccia, Adv. Funct. Mater. **25**, 5650 (2015).
[44] B. Abdollahi Nejand, V. Ahmadi, and H. R. Shahverdi, ACS Appl. Mater. Interfaces **7**, 21807 (2015).
[45] Z. Yu and L. Sun, Adv. Energy Mater. **5**, 1500213 (2015).
[46] D. Bi, W. Tress, M. I. Dar, P. Gao, J. Luo, C. Renevier, K. Schenk, A. Abate, F. Giordano, J.-P. Correa Baena, J.-D. Decoppet, S. M. Zakeeruddin, M. K. Nazeeruddin, M. Gratzel, and A. Hagfeldt, Sci. Adv. **2**, e1501170 (2016).
[47] W. S. Yang, J. H. Noh, N. J. Jeon, Y. C. Kim, S. Ryu, J. Seo, and S. I. Seok, Science **348**, 1234 (2015).
[48] J. Dong, Y. Zhao, J. Shi, H. Wei, J. Xiao, X. Xu, J. Luo, J. Xu, D. Li, Y. Luo, and Q. Meng, Chem. Commun. **50**, 13381 (2014).
[49] S. Guarnera, A. Abate, W. Zhang, J. M. Foster, G. Richardson, A. Petrozza, and H. J. Snaith, J. Phys. Chem. Lett. **6**, 432 (2015).
[50] E. M. Sanehira, B. J. Tremolet de Villers, P. Schulz, M. O. Reese, S. Ferrere, K. Zhu, L. Y. Lin, J. J. Berry, and J. M. Luther, ACS Energy Lett. **1**, 38 (2016).
[51] W. Li, H. Dong, L. Wang, N. Li, X. Guo, J. Li, and Y. Qiu, J. Mater. Chem. A **2**, 13587 (2014).
[52] G. Niu, W. Li, F. Meng, L. Wang, H. Dong, and Y. Qiu, J. Mater. Chem. A **2**, 705 (2014).
[53] J. Cao, J. Yin, S. Yuan, Y. Zhao, J. Li, and N. Zheng, Nanoscale **7**, 9443 (2015).
[54] J. Zhang, Z. Hu, L. Huang, G. Yue, J. Liu, X. Lu, Z. Hu, M. Shang, L. Han, and Y. Zhu, Chem. Commun. **51**, 7047 (2015).
[55] H. Back, G. Kim, J. Kim, J. Kong, T. K. Kim, H. Kang, H. Kim, J. Lee, S. Lee, and K. Lee, Energy Environ. Sci. **9**, 1258 (2016).
[56] Y. Han, S. Meyer, Y. Dkhissi, K. Weber, J. M. Pringle, U. Bach, L. Spiccia, and Y.-B. Cheng, J. Mater. Chem. A **3**, 8139 (2015).
[57] Y. Kato, L. K. Ono, M. V. Lee, S. Wang, S. R. Raga, and Y. Qi, Adv. Mater. Interfaces **2**, 2 (2015).
[58] A. Guerrero, J. You, C. Aranda, Y. S. Kang, G. Garcia-Belmonte, H. Zhou, J. Bisquert, and Y. Yang, ACS Nano **10**, 218 (2015).
[59] F. Guo, H. Azimi, Y. Hou, T. Przybilla, M. Hu, C. Bronnbauer, S. Langner, E. Spiecker, K. Forberich, and C. J. Brabec, Nanoscale **7**, 1642 (2014).
[60] Z. Ku, Y. Rong, M. Xu, T. Liu, and H. Han, Sci. Rep. **3**, 3132 (2013).
[61] A. Mei, X. Li, L. Liu, Z. Ku, T. Liu, Y. Rong, M. Xu, M. Hu, J. Chen, Y. Yang, M. Grätzel, and H. Han, Science **345**, 295 (2014).
[62] Y. Rong, Z. Ku, A. Mei, T. Liu, M. Xu, S. Ko, X. Li, and H. Han, J. Phys. Chem. Lett. **5**, 2160 (2014).
[63] X. Xu, Z. Liu, Z. Zuo, M. Zhang, Z. Zhao, Y. Shen, H. Zhou, Q. Chen, Y. Yang, and M. Wang, Nano Lett. **15**, 2402 (2015).
[64] Y. Li, J. K. Cooper, R. Buonsanti, C. Giannini, Y. Liu, F. M. Toma, and I. D. Sharp, J. Phys. Chem. Lett. **6**, 493 (2015).
[65] H. Zhou, Y. Shi, K. Wang, Q. Dong, X. Bai, Y. Xing, Y. Du, and T. Ma, J. Phys. Chem. C **119**, 4600 (2015).
[66] X. Li, M. Tschumi, H. Han, S. S. Babkair, R. A. Alzubaydi, A. A. Ansari, S. S. Habib, M. K. Nazeeruddin, S. M. Zakeeruddin, and M. Grätzel, Energy Technol. **3**, 551 (2015).
[67] T. Leijtens, G. E. Eperon, S. Pathak, A. Abate, M. M. Lee, and H. J. Snaith, Nat. Commun. **4**, 2885 (2013).
[68] A. J. Pearson, G. E. Eperon, P. E. Hopkinson, S. N. Habisreutinger, J. T.-W. Wang, H. J. Snaith, and N. C. Greenham, Adv. Energy Mater. **6**, 1600014 (2016).
[69] D. Bryant, N. Aristidou, S. Pont, I. Sanchez-Molina, T. Chotchunangatchaval, S. Wheeler, J. R. Durrant, and S. A. Haque, Energy Environ. Sci. **9**, 1655 (2016).
[70] F. T. F. O'Mahony, Y. H. Lee, C. Jellett, S. Dmitrov, D. T. J. Bryant, J. R. Durrant, B. C. O'Regan, M. Graetzel, M. K. Nazeeruddin, and S. A. Haque, J. Mater. Chem. A **3**, 7219 (2015).
[71] N. Aristidou, I. Sanchez-Molina, T. Chotchuangchutchaval, M. Brown, L. Martinez, T. Rath, and S. A. Haque, Angew. Chem., Int. Ed. **54**, 8208 (2015).
[72] A. Fakharuddin, F. Di Giacomo, I. Ahmed, Q. Wali, T. M. Brown, and R. Jose, J. Power Sources **283**, 61 (2015).
[73] A. V Vinogradov, H. Zaake-Hertling, E. Hey-Hawkins, A. V. Agafonov, G. A. Seisenbaeva, V. G. Kessler, and V. V. Vinogradov, Chem. Commun. **50**, 10210 (2014).
[74] D. Bi, G. Boschloo, S. Schwarzmüller, L. Yang, E. M. J. Johansson, and A. Hagfeldt, Nanoscale **5**, 11686 (2013).
[75] T. L. Thompson and J. T. Yates, Top. Catal. **35**, 197 (2005).
[76] M. A. Henderson, Surf. Sci. Rep. **66**, 185 (2011).
[77] S. N. Habisreutinger, L. Schmidt-Mende, and J. K. Stolarczyk, Angew. Chem., Int. Ed. Engl. **52**, 7372 (2013).
[78] K. Wojciechowski, S. D. Stranks, A. Abate, G. Sadoughi, A. Sadhanala, N. Kopidakis, G. Rumbles, C. Li, R. H. Friend, A.K.-Y. Jen, and H. J. Snaith, ACS Nano **8**, 12701 (2014).
[79] K. Wojciechowski, T. Leijtens, S. Siprova, C. Schlueter, M. T. Hörantner, J. T. W. Wang, C. Z. Li, A. K. Y. Jen, T. L. Lee, and H. J. Snaith, J. Phys. Chem. Lett. **6**, 2399 (2015).
[80] W. Li, W. Zhang, S. Van Reenen, R. J. Sutton, J. Fan, A. Haghighirad, M. Johnston, L. Wang, and H. Snaith, Energy Environ. Sci. **9**, 490 (2016).
[81] S. K. Pathak, A. Abate, P. Ruckdeschel, B. Roose, K. C. Gödel, Y. Vaynzof, A. Santhala, S. I. Watanabe, D. J. Hollman, N. Noel, A. Sepe, U. Wiesner, R. Friend, H. J. Snaith, and U. Steiner, Adv. Funct. Mater. **24**, 6046 (2014).
[82] B. Roose, K. C. Gödel, S. Pathak, A. Sadhanala, J. P. C. Baena, B. D. Wilts, H. J. Snaith, U. Wiesner, M. Grätzel, U. Steiner, and A. Abate, Adv. Energy Mater. **6**, 1501868 (2016).
[83] I. Hwang and K. Yong, ACS Appl. Mater. Interfaces **8**, 4226 (2016).
[84] Z. Xiao, C. Bi, Y. Shao, Q. Dong, Q. Wang, Y. Yuan, C. Wang, Y. Gao, and J. Huang, Energy Environ. Sci. **7**, 2619 (2014).

[85] P. Docampo, J. M. Ball, M. Darwich, G. E. Eperon, and H. J. Snaith, Nat. Commun. **4**, 2761 (2013).
[86] H. Choi, C.-K. Mai, H.-B. Kim, J. Jeong, S. Song, G. C. Bazan, J. Y. Kim, and A. J. Heeger, Nat. Commun. **6**, 7348 (2015).
[87] F. Igbari, M. Li, Y. Hu, Z. Wang, and L.-S. Liao, J. Mater. Chem. A **4**, 1326 (2016).
[88] F. Hou, Z. Su, F. Jin, X. Yan, L. Wang, H. Zhao, J. Zhu, B. Chu, and W. Li, Nanoscale **7**, 9427 (2015).
[89] Z. K. Wang, M. Li, D. X. Yuan, X. B. Shi, H. Ma, and L. S. Liao, ACS Appl. Mater. Interfaces **7**, 9645 (2015).
[90] J.-S. Yeo, R. Kang, S. Lee, Y.-J. Jeon, N. Myoung, C.-L. Lee, D.-Y. Kim, J.-M. Yun, Y.-H. Seo, S.-S. Kim, and S.-I. Na, Nano Energy **12**, 96 (2014).
[91] J. H. Kim, P. W. Liang, S. T. Williams, N. Cho, C. C. Chueh, M. S. Glaz, D. S. Ginger, and A. K. Y. Jen, Adv. Mater. **27**, 695 (2015).
[92] F. Zhang, X. Yang, M. Cheng, W. Wang, and L. Sun, Nano Energy **20**, 108 (2016).
[93] O. Malinkiewicz, A. Yella, Y. H. Lee, G. M. Espallargas, M. Graetzel, M. K. Nazeeruddin, and H. J. Bolink, Nat. Photonics **8**, 128 (2013).
[94] J. You, L. Meng, T.-B. Song, T.-F. Guo, Y. (Michael) Yang, W.-H. Chang, Z. Hong, H. Chen, H. Zhou, Q. Chen, Y. Liu, N. De Marco, and Y. Yang, Nat. Nanotechnol. **11**, 1 (2015).
[95] J. Lewis, Mater. Today **9**, 38 (2006).
[96] F. C. Krebs, Sol. Energy Mater. Sol. Cells **90**, 3633 (2006).
[97] S. Schuller, P. Schilinsky, J. Hauch, and C. J. Brabec, Appl. Phys. A: Mater. Sci. Process. **79**, 37 (2004).
[98] I. Hwang, I. Jeong, J. Lee, M. J. Ko, and K. Yong, ACS Appl. Mater. Interfaces **7**, 17330 (2015).
[99] C.-Y. Chang, K.-T. Lee, W.-K. Huang, H.-Y. Siao, and Y.-C. Chang, Chem. Mater. **27**, 5122 (2015).
[100] H. C. Weerasinghe, Y. Dkhissi, A. D. Scully, R. A. Caruso, and Y. B. Cheng, Nano Energy **18**, 118 (2015).
[101] M. Grätzel and N. Park, Nano **09**, 1440002 (2014).
[102] X. Dong, X. Fang, M. Lv, B. Lin, S. Zhang, J. Ding, and N. Yuan, J. Mater. Chem. A **3**, 5360 (2015).
[103] J. Zhao, B. Cai, Z. Luo, Y. Dong, Y. Zhang, H. Xu, B. Hong, Y. Yang, L. Li, W. Zhang, and C. Gao, Sci. Rep. **6**, 21976 (2016).
[104] G. Niu, X. Guo, and L. Wang, J. Mater. Chem. A **3**, 8970 (2014).
[105] C. C. Stoumpos, C. D. Malliakas, and M. G. Kanatzidis, Inorg. Chem. **52**, 9019 (2013).
[106] F. C. Schaefer, J. Org. Chem. **27**, 3608 (1962).
[107] T. Baikie, Y. Fang, J. M. Kadro, M. Schreyer, F. Wei, S. G. Mhaisalkar, M. Graetzel, and T. J. White, J. Mater. Chem. A **1**, 5628 (2013).
[108] Y. Liu, Z. Yang, D. Cui, X. Ren, J. Sun, X. Liu, J. Zhang, Q. Wei, H. Fan, F. Yu, X. Zhang, C. Zhao, and S. F. Liu, Adv. Mater. **27**, 5176 (2015).
[109] B. Conings, J. Drijkoningen, N. Gauquelin, A. Babayigit, J. D'Haen, L. D'Olieslaeger, A. Ethirajan, J. Verbeeck, J. Manca, E. Mosconi, F. De Angelis, and H. Boyen, Adv. Energy Mater. **5**, 1500477 (2015).
[110] J. H. Noh, S. H. Im, J. H. Heo, T. N. Mandal, and S. Il Seok, Nano Lett. **13**, 1764 (2013).
[111] Y. Chen, B. Li, W. Huang, D. Gao, and Z. Liang, Chem. Commun. (Cambridge) **51**, 11997 (2015).
[112] Y. Iwadate, K. Kawamura, K. Igarashi, and J. Mochinaga, J. Phys. Chem. **86**, 5205 (1982).
[113] A. Halder, R. Chulliyil, A. S. Subbiah, T. Khan, S. Chattoraj, A. Chowdhury, and S. K. Sarkar, J. Phys. Chem. Lett. **6**, 3483 (2015).
[114] Q. Jiang, D. Rebollar, J. Gong, E. L. Piacentino, C. Zheng, and T. Xu, Angew. Chem., Int. Ed. Engl. **54**, 7617 (2015).
[115] M. Daub and H. Hillebrecht, Angew. Chem. **127**, 11168 (2015).
[116] Q. Tai, P. You, H. Sang, Z. Liu, C. Hu, H. L. W. Chan, and F. Yan, Nat. Commun. **7**, 11105 (2016).
[117] A. M. Ganose, C. N. Savory, and D. O. Scanlon, J. Phys. Chem. Lett. **6**, 4594 (2015).
[118] I. C. Smith, E. T. Hoke, D. Solis-Ibarra, M. D. McGehee, and H. I. Karunadasa, Angew. Chem. **126**, 11414 (2014).
[119] D. H. Cao, C. C. Stoumpos, O. K. Farha, J. T. Hupp, and M. G. Kanatzidis, J. Am. Chem. Soc. **137**, 7843 (2015).
[120] N. J. Jeon, J. H. Noh, W. S. Yang, Y. C. Kim, S. Ryu, J. Seo, and S. Il Seok, Nature **517**, 476 (2015).
[121] N. Pellet, P. Gao, G. Gregori, T.-Y. Yang, M. K. Nazeeruddin, J. Maier, and M. Grätzel, Angew. Chem., Int. Ed. **53**, 3151 (2014).
[122] G. E. Eperon, S. D. Stranks, C. Menelaou, M. B. Johnston, L. Herz, and H. Snaith, Energy Environ. Sci. **7**, 982 (2014).
[123] G. E. Eperon, G. M. Paterno', R. J. Sutton, A. Zampetti, A. Haghighirad, F. Cacialli, and H. Snaith, J. Mater. Chem. A **3**, 19688 (2015).
[124] R. J. Sutton, G. E. Eperon, L. Miranda, E. S. Parrott, B. A. Kamino, J. B. Patel, M. T. Hörantner, M. B. Johnston, A. A. Haghighirad, D. T. Moore, and H. J. Snaith, Adv. Energy Mater. **6**, 1502458 (2016).
[125] M. Kulbak, S. Gupta, N. Kedem, I. Levine, T. Bendikov, G. Hodes, and D. Cahen, J. Phys. Chem. Lett. **7**, 167 (2016).
[126] R. E. Beal, D. J. Slotcavage, T. Leijtens, A. R. Bowring, R. A. Belisle, W. H. Nguyen, G. F. Burkhard, E. T. Hoke, and M. D. McGehee, J. Phys. Chem. Lett. **7**, 746 (2016).
[127] D. P. McMeekin, G. Sadoughi, W. Rehman, G. E. Eperon, M. Saliba, M. T. Hörantner, A. Haghighirad, N. Sakai, L. Korte, B. Rech, M. B. Johnston, L. M. Herz, and H. J. Snaith, Science **351**, 151 (2016).
[128] J.-W. Lee, D.-H. Kim, H.-S. Kim, S.-W. Seo, S. M. Cho, and N.-G. Park, Adv. Energy Mater. **5**, 1501310 (2015).
[129] Z. Li, M. Yang, J.-S. Park, S.-H. Wei, J. Berry, and K. Zhu, Chem. Mater. **28**, 284 (2015).
[130] C. Yi, J. Luo, S. Meloni, A. Boziki, N. Ashari-Astani, C. Grätzel, S. M. Zakeeruddin, U. Rothlisberger, and M. Grätzel, Energy Environ. Sci. **9**, 656 (2015).
[131] A. Binek, F. C. Hanusch, P. Docampo, and T. Bein, J. Phys. Chem. Lett. **6**, 1249 (2015).
[132] J.-W. Lee, D.-J. Seol, A.-N. Cho, and N.-G. Park, Adv. Mater. **26**, 4991 (2014).
[133] T. M. Koh, K. Fu, Y. Fang, S. Chen, T. C. Sum, N. Mathews, S. G. Mhaisalkar, P. P. Boix, and T. Baikie, J. Phys. Chem. C **118**, 16458 (2014).
[134] M. Kulbak, D. Cahen, and G. Hodes, J. Phys. Chem. Lett. **6**, 2452 (2015).
[135] C. C. Stoumpos, C. D. Malliakas, J. A. Peters, Z. Liu, M. Sebastian, J. Im, T. C. Chasapis, A. C. Wibowo, D. Y. Chung, A. J. Freeman, B. W. Wessels, and M. G. Kanatzidis, Cryst. Growth Des. **13**, 2722 (2013).
[136] Q. Ma, S. Huang, X. Wen, M. A. Green, and A. W. Y. Ho-Baillie, Adv. Energy Mater. **6**, 1502202 (2016).